Earth and Planetary Science Letters 351–352 (2012) 134–146

Contents lists available at SciVerse ScienceDirect

Earth and Planetary Science Letters

journal homepage: www.elsevier.com/locate/epsl

Linking continental drift, plate tectonics and the thermal state of the Earth's mantle

T. Rolf [a,*], N. Coltice [b,c], P.J. Tackley [a]

[a] Institute of Geophysics, Department of Earth Sciences, ETH Zurich, Switzerland, Sonneggstrasse 5, 8092 Zurich, Switzerland
[b] Laboratoire de Géologie de Lyon, Université Claude Bernard Lyon 1, Ecole Normale Supérieure de Lyon, CNRS, France
[c] Institut Universitaire de France, France

ARTICLE INFO

Article history:
Received 2 December 2011
Received in revised form
26 June 2012
Accepted 7 July 2012
Editor: T. Spohn
Available online 30 August 2012

Keywords:
thermal history
plate tectonics
continents
thermal insulation
mantle convection

ABSTRACT

Continents slowly drift at the top of the mantle, sometimes colliding, splitting and aggregating. The evolutions of the continent configuration, as well as oceanic plate tectonics, are surface expressions of mantle convection and closely linked to the thermal state of the mantle; however, quantitative studies are so far lacking. In the present study we use 3D spherical numerical simulations with self-consistently generated plates and compositionally and rheologically distinct continents floating at the top of the mantle in order to investigate the feedbacks between continental drift, oceanic plate tectonics and the thermal state of the Earth's mantle, by using different continent configurations ranging from one supercontinent to six small continents. With the presence of a supercontinent we find a strong time-dependence of the oceanic surface heat flow and suboceanic mantle temperature, driven by the generation of new plate boundaries. Very large oceanic plates correlate with periods of hot suboceanic mantle, while the mantle below smaller oceanic plates tends to be colder. Temperature fluctuations of subcontinental mantle are significantly smaller than in oceanic regions and are caused by a time-variable efficiency of thermal insulation of the continental convection cell. With the presence of multiple continents the temperature below individual continents is generally lower than below supercontinent and is more time-dependent, with fluctuations as large as 15% that are caused by continental assembly and dispersal. The periods featuring a hot subcontinental mantle correlate with strong clustering of the continents and periods characterized by cold subcontinental mantle, at which it can even be colder than suboceanic mantle, with a more dispersed continent configuration. Our findings with multiple continents imply that periods of partial melting and strong magmatic activity inside the continents, which may contribute to continental rifting and pronounced growth of continental crust, might be episodic processes related to the supercontinent cycle. Finally, we observe an influence of continents on the wavelength of convection: for a given strength of the lithosphere we observe longer-wavelength flow components, when continents are present. This observation is regardless of the number of continents, but most pronounced for a single supercontinent.

1. Introduction

In 1931 Arthur Holmes proposed that continental drift and seafloor kinematics are surface expressions of large-scale convection in the mantle. Plate reconstructions support this hypothesis: for instance, the closure of the Tethys ocean happened as the Indian continental block moved northwards at a very high velocity, under the influence of hot mantle structures (Cande and Stegman, 2011) and subduction at the Tethyan trench. The influence of continental drift on mantle convection could be at the origin of geoid highs in the Atlantic, as they are possibly caused by insulation by the Pangaean supercontinent assembly during the Mesozoic (Anderson, 1982). Enhanced magmatic activity may have influenced continental break-up and dispersal of the fragments, but long-lived thermal anomalies still remain stable at the former site of continental insulation.

Numerical simulations and laboratory experiments have confirmed that the dynamic feedback between continents and mantle convection is fundamental. Although continents do not actively take part in the convective mantle overturn, they influence the convective flow by imposing long-wavelength flow components (Gurnis, 1988; Zhong and Gurnis, 1993; Guillou and Jaupart, 1995; Lowman and Gable, 1999; Yoshida et al., 1999; Phillips and Bunge, 2005; Grigné et al., 2007; Zhong et al., 2007) and insulating the convecting mantle (Lenardic and Moresi, 2001; Lenardic et al., 2005; Cooper et al., 2006). The change in the temperature field

* Corresponding author. Tel.: +41 446337653.
E-mail address: Tobias.Rolf@erdw.ethz.ch (T. Rolf).

0012-821X/$ - see front matter © 2012 Elsevier B.V. All rights reserved.
http://dx.doi.org/10.1016/j.epsl.2012.07.011

consequently modifies the body forces that drive the motion of continental blocks.

The principal aspects of the dynamic feedback between mantle convection and continents have been investigated and described, but very few studies propose a quantitative framework that allows comparison with geological observations and detailed convection characteristics. Recently, on the basis of 3D spherical models Coltice et al. (2007, 2009) and Phillips and Coltice (2010) proposed a theory in which the evolution of the distribution of continents at the Earth's surface causes temperature changes of 50–100 K. Geological observations support this hypothesis. For instance, the Central Atlantic Magmatic Province was emplaced when continents were aggregated to form Pangaea. It is associated with a broad subcontinental temperature increase since no evidence of a hotspot track or significant uplift has been found (McHone, 2000).

Describing the feedbacks between mantle convection, plate tectonics, and continental drift is of fundamental importance but requires state-of-the-art modeling. Yet, Coltice et al. (2009) and Phillips and Coltice (2010) simplified their model by assuming constant or at most layered viscosity without any temperature dependence, such that the resulting temperature difference between suboceanic and subcontinental mantle might be overestimated. A weakly temperature-dependent viscosity was used by Zhong et al. (2007) and Zhang et al. (2009), but in order to model Earth-like plate tectonics a stronger temperature dependence and a weakening mechanism like plastic yielding are necessary. Following earlier models in 2D cartesian geometry (e.g. Lenardic et al., 2003; O'Neill et al., 2008), Yoshida (2010) first presented a 3D spherical model with self-consistent plate tectonics and continents, but could model only a part of the sphere, which does not capture long-wavelength flow components, and a relatively short integration time. Recently, a global spherical model was introduced by Rolf and Tackley (2011), who investigated the influence of a single continent on plate-like behavior and found that continents strongly influence the regime of convection, thus wavelength and heat budget of the mantle.

Here we extend the model of Rolf and Tackley (2011) to multiple continent simulations and investigate how continental drift, seafloor tectonics and mantle convection interact in an environment similar to Earth-like plate tectonics. We analyse how plate configurations and continental distribution influence the temperature of the oceanic and continental mantle. In the next section we start with a brief description of our numerical model (Section 2), followed by details about the calculations performed and the results we have obtained (Section 3). Afterwards we discuss our results, integrate them into the geophysical context (Section 4) and finally summarize the key aspects in Section 5.

2. Numerical model

Our intention here is to study the coupled tectonic and thermal evolution of the mantle-continent system. We consider here a first order view of that problem: mantle convection is driven by the sinking of cold plates, while continents mostly resist subduction due to their different composition. Hence, we model mantle convection interacting with continents by convection of an incompressible viscous material with a rheology that generates plate-like behavior, heated from within. The material is compositionally heterogeneous since continents are lighter and more viscous than the mantle. Therefore, a non-diffusive compositional field C is introduced to model the continents. These are simplified as homogeneous Archaean cratons, with $C=1$ representing pure continental and $C=0$ pure non-continental material. After advection some continental material can get entrained into the mantle, thus C is a continuous field between 0 and 1. After being initialized, the cratons are treated self-consistently, which means they differ from normal mantle material only in terms of physical properties. The compositional field is tracked using the tracer-ratio method (Tackley and King, 2003). This modeling is described in Rolf and Tackley (2011).

The governing non-dimensional equations for Boussinesq, incompressible thermo-chemical convection are

$$\vec{\nabla}\cdot\vec{u}=0 \tag{1}$$

$$-\vec{\nabla}P+\vec{\nabla}\cdot[\eta(\partial_i u_j+\partial_j u_i)]=Ra(T-RC)\vec{e_r} \tag{2}$$

$$\partial_t T+\vec{u}\cdot\vec{\nabla}T=\nabla^2 T+H \tag{3}$$

$$\partial_t C+\vec{u}\cdot\vec{\nabla}C=0 \tag{4}$$

where $\vec{u}$, P, η, T, C, $\vec{e_r}$ and t represent velocity, pressure, viscosity, temperature, composition, radial unit vector and time, respectively. The three controlling parameters are the internal heating rate H, the buoyancy ratio R, which is the ratio of the density difference $\Delta\rho$ of continental material to the thermal density variation $\rho_0\alpha_0\Delta T$, and the Rayleigh number $Ra=\alpha_0 g_0 D^3 \Delta T\rho_0/\kappa_0\eta_0$. In these definitions ρ_0 is a reference density, α_0 the thermal expansivity, ΔT the temperature drop across the lithosphere, g_0 the gravitational acceleration, D the mantle thickness, κ_0 the thermal diffusivity and η_0 a reference viscosity obtained at $T=1$. The values of the various parameters used here are given in Table 1.

In addition to a density contrast (controlled by the buoyancy ratio R), continental and oceanic material have different viscosities and yield strengths. The viscosity is given by

$$\eta_T(T,C)=\exp[\ln(\Delta\eta_C)C]\cdot\exp\left[\frac{\tilde{E}_A}{T+1}-\frac{\tilde{E}_A}{2}\right] \tag{5}$$

where $\Delta\eta_C=\eta(T,C=1)/\eta(T,C=0)$ accounts for the compositional dependence and $\tilde{E}_A$ is the activation energy that accounts for the temperature dependence of the viscosity. Here, $\tilde{E}_A$ is a constant and set to 23.03, which gives five orders of magnitude viscosity variation in the interval $0\le T\le 1$. This is sufficient for the formation of a stagnant lid covering the mantle (Solomatov, 1995). Plastic yielding is assumed to be the weakening mechanism that is necessary to break the stagnant lid and obtain Earth-like plate tectonics (Moresi and Solomatov, 1998; Tackley, 2000a).

Table 1
Symbols, definitions and values of the non-dimensional and dimensional parameters used in this study. As a lower than Earth-like Rayleigh number is used here, one of the parameters in the definition of the Rayleigh number has to differ from its estimation for the present-day Earth's mantle: in this case the viscosity is assumed to be higher as it is the parameter with the highest uncertainty.

Symbol	Definition	Value	Unit
Ra_0	Rayleigh number	1.0×10^6	–
H	Internal heating rate	20.5	–
σ_Y^0	Surface yield stress	1.0×10^4	–
σ_Y'	Yield stress gradient	2.0×10^5	–
R	Buoyancy ratio	-0.4	–
$\Delta\sigma_Y$	Comp. yield stress contrast	10	–
$\Delta\eta_C$	Comp. viscosity contrast	100	–
α_0	Thermal expansivity	3.0×10^{-5}	K^{-1}
g_0	Grav. acceleration	10.0	$m\,s^{-2}$
D	Mantle thickness	2.89×10^6	m
ΔT	Temperature drop	1300	K
T_S	Surface temperature	300	K
ρ_0	Reference density	3300	$kg\,m^{-3}$
k_0	Thermal conductivity	3.15	$W\,m^{-1}\,K^{-1}$
κ_0	Thermal diffusivity	1.0×10^{-6}	$m^2\,s^{-1}$
η_0	Reference viscosity	3.1×10^{22}	Pa s

The yield stress, which is the maximum stress the material can resist before deforming plastically, is defined by

$$\sigma_Y(d,C) = \exp[\ln(\Delta\sigma_Y)C] \cdot (\sigma_Y^0 + d \cdot \sigma_Y') \quad (6)$$

where $\Delta\sigma_Y = \sigma_Y(d,C=1)/\sigma_Y(d,C=0)$ accounts for different yield stresses of cratonic and oceanic lithosphere. $\sigma_Y^0 = \sigma_Y(d=0,C=0)$ is the yield stress at the oceanic surface. It increases linearly with increasing depth d at a rate of σ_Y'. If the convective stress exceeds the yield stress, the viscosity is reduced to the yielding viscosity $\eta_Y = \sigma_Y/2\dot{\epsilon}$, where $\dot{\epsilon}$ is the 2nd invariant of the strain-rate tensor. The effective viscosity is then given by $\eta_e = [\eta_T^{-1} + \eta_Y^{-1}]^{-1}$.

The numerical models in this study are computed in 3D spherical geometry on a Yin-Yang grid (Tackley, 2008) with a resolution of $64 \times 192 \times 32 \times 2$ cells and an average of 12.7 tracers per cell. The radial grid spacing is refined in the surface boundary layer. One case was run with a resolution of $128 \times 384 \times 64 \times 2$ and did not show significant changes. All cases have a reference Rayleigh number $Ra_0 = 10^6$, which is defined by a non-dimensional reference viscosity of 1 (obtained at $T=1$). Using the parameter values in Table 1 this corresponds to a dimensional reference viscosity of $\eta_0 \approx 3.1 \times 10^{22}$ Pa s. The heat input in these models comes from internal heat sources only ($H = 20.5$, $H_{dim} \approx 3 \times 10^{-12}$ W kg^{-1}), i.e. the bottom boundary is insulating. Accordingly the Rayleigh number based on internal heating is $Ra_H = Ra_0 \cdot H \approx 2 \times 10^7$, which is (due to computational costs) less than that estimated for the Earth mantle: $Ra_H^E = \mathcal{O}(10^9)$ (Turcotte and Schubert, 2002). Because these models do not generate hot plumes, they emphasize the effects of the top boundary layer dynamics on the global thermal evolution. For simplicity, a viscosity increase with depth owing to the phase change that defines the lower mantle is not considered here. The top and bottom boundaries are free-slip.

In order to ensure that all cases are in the plate-like mode of convection, the yield stress of normal mantle material is set to a surface value of ≈ 37 MPa, which increases with depth at a rate of ≈ 0.26 MPa km^{-1}. These stresses are dimensionalized with a factor $\eta_0\kappa_0/D^2$ (see Table 1). The longevity of continental lithosphere is assured by (1) a density difference between continental material and normal mantle of about -50 kg m^{-3} ($R = -0.4$), which is only slightly smaller than inferred from experiments on peridotite xenoliths (Poudjom Djomani et al., 2001), and (2) increased viscosity and yield stress of continental material ($\Delta\eta_C = 100$, $\Delta\sigma_Y = 10$), which might be explained by the relative dehydration of cratonic lithosphere (Hirth and Kohlstedt, 1996; Karato, 2010) and follows results from various earlier modeling studies (e.g. O'Neill et al., 2008).

To improve plate-like behavior we use a low-viscosity asthenosphere following the implementation of Tackley (2000b), in which the viscosity of material hotter than its solidus is decreased by a constant factor $\Delta\eta_M = 0.1$. The depth-dependent solidus is calculated using $T_{sol}(d) = T_{sol}(0) + d \cdot T_{sol}'$, where $T_{sol}(0) = 0.6$ is the surface value and $T_{sol}' = 2.0$ is the rate of increase with increasing depth. These non-dimensional parameters approximately correspond to 1160 K and 1 K km^{-1}.

3. Simulations and results

In our set of simulations we use different continent configurations ranging from one supercontinent covering 30% of the

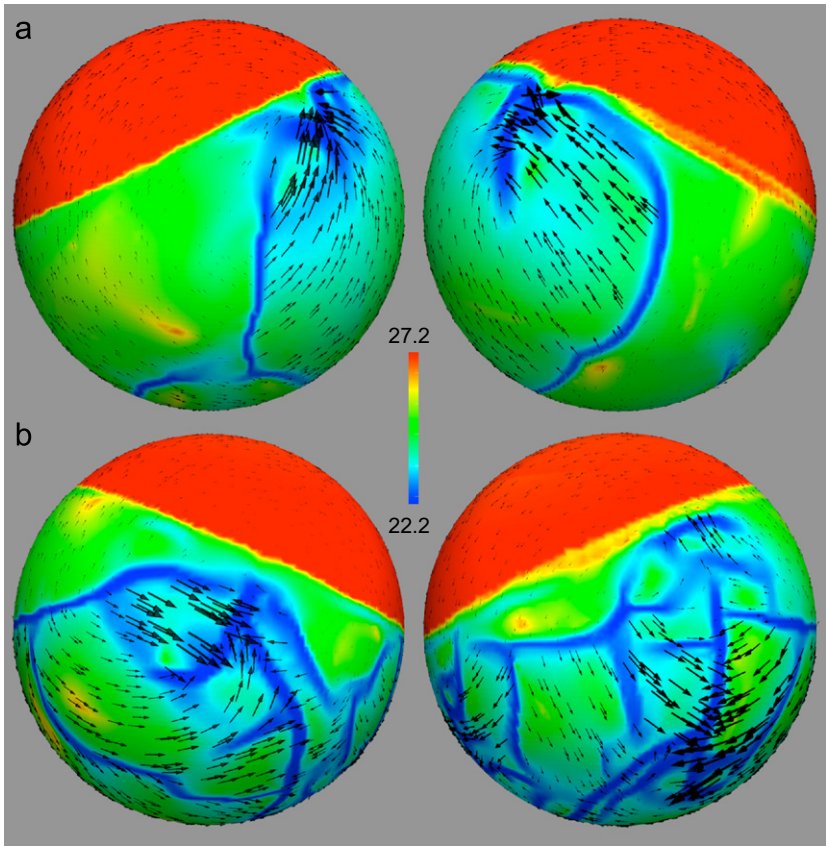

Fig. 1. Snapshots of the supercontinent case. Shown is the viscosity field for front (left) and back half (right) of the sphere for two different points in time: (a) $t_A \approx 2.45$ Ga and (b) $t_B \approx 2.64$ Ga. Red represents the highly viscous continent, green the oceanic plates and blue the weak plate boundaries. The colorbar defines values of the decadic logarithm in Pa s. Viscosities have been scaled with the reference viscosity $\eta_0 = \alpha_0 g_0 \Delta T D^3 \rho_0/\kappa_0 Ra_0$ given in Table 1, such that $\eta_{dim} = \eta \cdot \eta_0$. Black arrows indicate the surface velocity field, where the arrow size scales with the magnitude of the velocity.

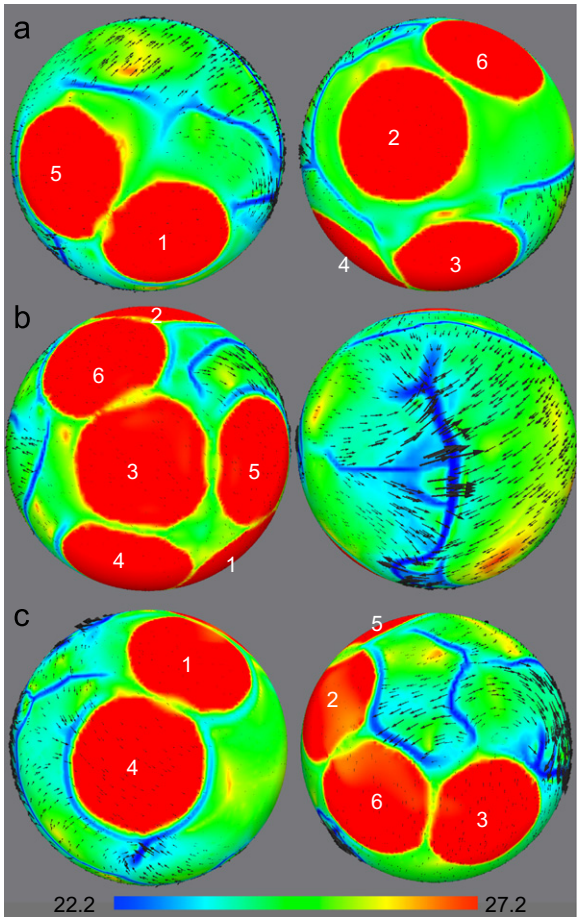

Fig. 2. As Fig. 1, but for the case with six smaller continents for times (a) $t_A \approx 1.3$ Ga, (b) $t_B \approx 3.6$ Ga and (c) $t_C \approx 4.4$ Ga. The white number labels identify different continents in subsequent figures.

surface (Fig. 1) to six smaller continents with 5% coverage each (Fig. 2). Except for a reference case without continents, the total continental coverage is kept constant at a value of 30%, which is a reasonable approximation for present-day Earth. The initial thickness of the continental roots is fixed to 20% of the mantle thickness ($\approx$570 km), because it is scaled with the Rayleigh number to obtain a realistic thickness ratio of continental to oceanic lithosphere (see Rolf and Tackley, 2011). As our goal is to study the physics of controlled continental configurations, the model does not allow for the production of new continental material by e.g. complex melting processes.

Initially we prescribe a linear geotherm inside the continents; this forces the continents to be initially colder than their surroundings. The models are run with the continents being fixed in position until a statistically steady-state is reached, after which continents are allowed to drift over the surface.

3.1. Supercontinent

We first concentrate on the configuration with only one supercontinent. Fig. 3a displays the temporal evolution of the average temperature below the continent and below the oceanic part. Here (and in all subsequent discussion) the subcontinental temperature refers to the temperature at the base of the continental thermal boundary layer and the suboceanic temperature is the temperature at the base of oceanic boundary layer. The base of the boundary layer is derived from the laterally averaged temperature profile by using the profile's maximum, which occurs under the plates in all calculations (Fig. A1 in Appendix). As continental plates are thicker than oceanic plates, subcontinental and suboceanic temperatures are usually not calculated at the same depth. Overall, the temperature below the supercontinent is higher than below the oceans, which is in good agreement with e.g. Phillips and Coltice (2010). On average, subcontinental mantle is $\approx$95 K hotter, but at times the difference can be more than 140 K (Fig. 3a).

Fig. 1 displays two snapshots of the surface velocities and viscosities, where the highest viscosity (red) corresponds to continental material and the lowest (blue) to regions where yielding occurs (plate boundaries). These snapshots represent the two end-member configurations that are observed in the simulation. The first one (top row, time t_A) is characterized by very few plate boundaries in the oceanic part of the model, i.e. few, but large tectonic plates. In the second one (bottom row, time t_B), many new plate boundaries have formed, hence the number of oceanic plates is larger, but the average plate size is smaller. The two plate configurations shown in Fig. 1 correspond to significant differences in the temperature distribution in this model. At time $t_A \approx 2.45$ Ga (with large plates) the subcontinental temperature is at a relative minimum, while the suboceanic temperature is very high and only $\approx$30 K lower than below the supercontinent (Fig. 3a). On the other hand at time $t_B \approx 2.65$ Ga the subcontinental temperature is very high and the suboceanic one is much ($\approx$145 K) lower.

The transition from one end-member configuration to another is correlated with changes of the thermal field. For instance, Lowman et al. (2001) as well as Grigné et al. (2005) showed that the heat transport efficiency of mantle convection decreases with increasing convective wavelength, consistent with Lenardic et al. (2005) and Phillips and Coltice (2010), who proposed that increased wavelength of convection and/or higher degrees of insulation raise the internal temperature. However, in our models, the typical length scale of convection varies with time as the number and size of plates change, hence insulation changes too, because it is controlled by the ratio of the continental area to the total area of a convection cell.

For the purely oceanic convection cells there is no continental insulation, thus, the wavelength effect controls the temperature in these cells. At time t_A the wavelength is large, i.e. only few plate boundaries exist and a limited number of downwellings cool the material in the interior. Consequently, the average oceanic heat flow is small (Fig. 3b) and the convection cell starts heating up. As oceanic plates grow, they become thicker and finally unstable, which results in the formation of new instabilities generating new plate boundaries and fragmenting plates in our model. This allows heat to escape more efficiently from the suboceanic mantle, such that the heat flux through the oceanic surface can drastically increase and its average temperature can decrease by up to 90 K on a relatively short timescale of about 100–150 Ma. This is in good agreement with the results of Gait and Lowman (2007), who found a similar increase of surface heat flux in comparable periods of time using a large aspect ratio 2D cartesian model with evolving kinematic oceanic plates, but no continents. Stein and Lowman (2010) also reported a strong coupling of surface heat flux with the evolution of plate number and plate size in a 3D cartesian model. In both of these studies, basal heating of the mantle was considered. Despite the different heating mode compared to the present study the heat flux observations are very similar, which possibly implies that plumes do not have a strong effect on the temporal variability of the surface heat flow when plates are present.

Although the number and size of oceanic plates change between the two configurations shown in Fig. 1a and b, the large-scale convective flow is always dominated by very long wavelength components. This can easily be seen by decomposing

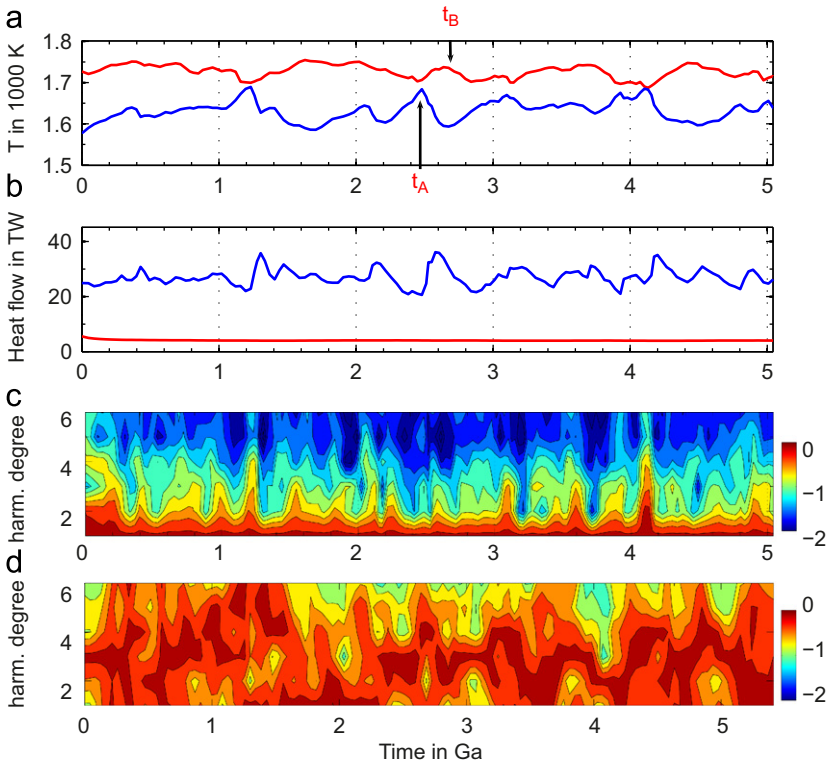

Fig. 3. (a) Time series of subcontinental (red) and suboceanic (blue) temperature for the case with a single continent, calculated at the base of the thermal boundary layer. t_A and t_B indicate when the configurations shown in Fig. 1 occur. Time is dimensionalized by scaling the model transit time τ_M to the one of the present-day Earth's mantle ($\tau_E = 85$ Ma), thus $t_{dim} = t \cdot \tau_E/\tau_M$. The point of time origin is defined by the time when continents start to move. For dimensionalization of temperatures and heat flows see the caption of Table 2. (b) Time series of the mean heat flow separated in continental (red) and oceanic part (blue). (c) Heterogeneity spectrogram of the temperature field versus time. Shown are the logarithmic powers ($\log_{10}$) of the first six harmonic degrees depth-averaged over the upper mantle. For each point in time the spectrum is normalized separately by the maximum spectral power occurring at this time. (d) As in (c), but for a reference case without a continent. Besides that, convection parameters are identical to the cases with continents. Here, the point of time origin is defined arbitrarily after the transient period. (For interpretation of the references to color in this figure caption, the reader is referred to the web version of this article.)

the temperature field into spherical harmonics. Fig. 3c displays the spectral amplitudes of the six lowest harmonic degrees. Despite temporal changes in the flow pattern, the first harmonic degree dominates throughout the entire calculation and variations in plate configuration only lead to more significant contributions of the higher harmonic degrees (here mainly degrees 2 and 3). In many cases this onset of shorter wavelength convection is followed by an increase in oceanic heat flow (which can be as high as 45%), most prominent in Fig. 3b at times $t \approx 1.2$ Ga and $t \approx 4.1$ Ga. However, these variations cannot break the overall degree 1 pattern.

The observation of this very long wavelength convection is consistent with previous results of e.g. Gurnis and Zhong (1991), Zhong and Gurnis (1993), Yoshida et al. (1999), Phillips and Bunge (2005), Zhong et al. (2007), Zhang et al. (2009), who found that the presence of a supercontinent imposed a degree 1 structure. In principle, the long wavelength structure could also be generated by the mantle itself, as reported by e.g. Chapman et al. (1980), Tackley (1996), McNamara and Zhong (2005), Yoshida (2008), Hoeink and Lenardic (2010). However, a case without continents, but with identical convection parameters shows that the spectral energy is much more distributed without a continent and the spectrum is more time-dependent (Fig. 3d). Thus, a dominance of the first harmonic degree is not observed. On the contrary, the higher order harmonics (up to degree 5) are prevalent instead. However, this observation could depend on the yielding properties of oceanic lithosphere: increasing its yield strength may lead to longer-wavelength convection even without the presence of a continent (van Heck and Tackley, 2008).

In contrast to the oceanic area, the heat flow through the thick continental lid is very small and quasi-constant in time. Thus, the variations in subcontinental temperature cannot be correlated with it. However, they can be explained by changes in the aspect ratio of the continental convection cell. At time t_A the plate boundaries in the oceans are relatively far away from the continental margin, such that the continental cell has a large aspect ratio and contains some amount of oceanic seafloor where cooling is more effective. According to the scalings of Lenardic et al. (2005) and Phillips and Coltice (2010) thermal insulation in this convection cell will be less efficient than at time t_B, when the continent is almost entirely surrounded by plate boundaries and the continental cell hardly contains oceanic seafloor. Furthermore, at time t_A heat can escape from the subcontinental mantle to the suboceanic mantle of the same convection cell, which leads to lower subcontinental temperatures than at time t_B, when the heat is captured below the continent. However, temperature variations below the continent are smaller than in the oceanic part and do not exceed 4% or 70 K.

3.2. *Multiple continents*

The supercontinent we used in the previous section was idealized as it was imposed as one uniform compact block. However, supercontinents in Earth's history formed by aggregation at a convergent plate boundary, i.e. an anomalously cold region of the mantle that ultimately warms up after continent assembly (e.g. Santosh et al., 2009). In order to investigate such a scenario we now consider multiple continents that can assemble

and disperse, instead of one imposed supercontinent. Variations of the continent configuration with time are likely to have a strong influence on the temperature distribution in the mantle (e.g. Anderson, 1982; Guillou and Jaupart, 1995; Lowman and Jarvis, 1995; Lowman and Gable, 1999; Trubitsyn et al., 2003; Coltice et al., 2007; Heron and Lowman, 2011). Here we used six different initial configurations with a constant total continental coverage of 30% (Table 2), but a varying number and diameter of continents to investigate the effect of changes in continent configuration on the evolution of suboceanic temperature and heat flow, as well as the difference between subcontinental and suboceanic temperatures.

A noteworthy observation in these simulations is that the assembled continent configuration is much more frequently observed than the dispersed configuration. An extreme example is the case with two continents of different sizes (covering 20% and 10% of the surface area): the two continental blocks assemble after 200–300 Ma and then never disperse again within a time span of 4 Ga. The difficulty of splitting assembled continents is observed in many of our simulations, but splitting appears to be easier the more continents are present, possibly because it is easier to generate short-wavelength flow structures, which might be necessary for the existence of dispersed continental blocks (Zhang et al., 2009). But it could also be possible that the size of individual continents is a relevant parameter for continental splitting. Furthermore, the rheology assumed in this study is not dependent on damage or history. Adding these complexities to our model could have important effects on the splitting of continents as former sites of continental collision might be weaker and heal only slowly with time.

However, in the present study we are mostly interested in the thermal consequences of changes in continent configuration rather than explaining the dynamic control of these changes themselves. We find that suboceanic temperatures and heat flows are not significantly affected by the continent configuration, which is not surprising as the total continental coverage, i.e. the insulating area, remains constant. Slightly lower suboceanic temperature can be observed in cases with more fragmentation of continents, but the difference is not more than 2%.

In contrast, the difference between subcontinental and suboceanic temperatures decreases with stronger fragmentation of continents, i.e. from ≈ 90 K with a single supercontinent to ≈ 30 K with six small continents. Although the temporal fluctuations and therewith the standard derivation of this signal are relatively high in our simulations with three or more continents, our finding is consistent with the much simpler models without oceanic plates of Coltice et al. (2007) and indicates that a significant temperature excess is more likely below large continents, which might lead to partial melting below these continents (Anderson, 1982). This is also supported by our two simulations in which continents with varying sizes are considered. As continents barely deform in these simulations, individual continents can be tracked throughout the whole evolution. Hence, subcontinental temperatures can be computed separately for each continent. In the case with two continents covering 20% and 10% of the surface, respectively, the mantle below the larger continent is more than 100 K hotter (on average) than the mantle below the smaller continent. Similar observations can be made in the case with three continents covering 15%, 10% and 5%, respectively.

The temperature excesses below continents described so far are affected by the different initial diameter of individual continents. However, in the course of a supercontinent cycle continental fragments will naturally have varying sizes, such that we will focus on the simulation with six identical continents (each covering 5% of the surface) in the following sections to describe the link between continent configuration and the thermal state of the mantle.

In this simulation (a movie is presented in the supplementary online material), the suboceanic temperature shows smaller variations than it does in the supercontinent case. The fluctuations of the subcontinental temperature can be interpreted in terms of three end-member continent configurations displayed in Fig. 2: (i) the dispersed state, for instance at time $t_A \approx 1.3$ Ga (Fig. 2a), where continents build three pairs or are more dispersed, (ii) the compact state at time $t_B \approx 3.6$ Ga (Fig. 2b), which is similar to the supercontinent state, and (iii) the chain-like state at time $t_C \approx 4.4$ Ga (Fig. 2c), where all continents are indeed connected, but form an elongated chain.

In Fig. 4a the temporal evolution of suboceanic temperature and the temperature below all individual continents is displayed. Consistent with e.g. Phillips and Coltice (2010) and our data given in Table 2, the average subcontinental temperatures are lower than in the supercontinent case (compare to Fig. 3a). Additionally, temporal variations in the temperature below individual continents as high as 15% (≈ 260 K) are observed. Sometimes the temperature below a continent is lower than that below oceans, especially for the continents that are located at the end of a chain structure (Fig. 2c). Furthermore, variations of suboceanic temperature and oceanic heat flow are smaller than in the supercontinent configuration ($\leq 5\%$ and $\leq 30\%$, respectively, see Fig. 4a and b) and the heterogeneity spectrogram (Fig. 4c) shows a more distributed spectral energy than in the supercontinent case (although still longer-wavelength than the no-continent case) with an alternating dominance of the 1st, 2nd or (rarely) 3rd harmonic degree. Apparently, the clear link between variations in convective wavelength, oceanic heat flow and the resulting changes in suboceanic and subcontinental temperatures that we observed in the supercontinent case, is not observable in this multiple continent case. Most likely it is superposed by the effects of continental assembly and dispersal.

In order to analyze these effects in more detail, we first focus on two specific examples and then try to obtain a more general observation. The temperature below continent '3' in Fig. 2b is plotted as the orange line in Fig. 4a. At time $t_B \approx 3.6$ Ga the mantle below this continent is very hot; much hotter than the suboceanic mantle. This can be explained by the supercontinent configuration at time t_B. Continent '3' is located in the center of the supercontinent and surrounded by other continents ('4', '5' and '6' in Fig. 2b). The highly clustered continents protect each other

Table 2
Time-averaged temperature difference between the subcontinental and suboceanic mantle ($\overline{T_C - T_O}$), minima, mean values and maxima of the suboceanic temperature (T_O^{min},T_O^{mean},T_O^{max}) and oceanic heat flow (Q_O^{min},Q_O^{mean},Q_O^{max}) for the different continent configurations used in this study. Dimensional temperatures are obtained by scaling the corresponding non-dimensional temperature to the average suboceanic temperature of the $5\% \times 6$-case ($T_{ref} = 0.906$), such that $T_{dim} = \Delta T \cdot T/T_{ref} + T_S$. The lower convective vigor in our simulations leads to time scales, velocities and heat flows that differ from those in the Earth's mantle. Thus, we scale the transit time of the model τ_M to that of the present-day Earth's mantle τ_E, which is 85 Ma assuming an average surface velocity of 3.4 cm a^{-1}. This leads to the following dimensionalization of (oceanic) heat flows (Coltice et al., 2012): $Q_{O,dim} = qA_O k_0 \Delta T/(\overline{T_O}\sqrt{\kappa_0 \tau_E/\tau_M})$, where q is the averaged non-dimensional local heat flux, $\overline{T_O}$ the averaged non-dimensional suboceanic temperature and $A_O \approx 3.57 \times 10^{14}$ m^2 the area of the present-day oceans.

Configuration	$\overline{T_C - T_O}$ (K)	$T_O^{min}/T_O^{mean}/T_O^{max}$ (K)	$Q_O^{min}/Q_O^{mean}/Q_O^{max}$ (TW)
$30\% \times 1$	(93 ± 37)	1579/1633/1689	21/27/36
$20\% + 10\%$	(59 ± 39)	1588/1628/1692	21/27/36
$15\% \times 2$	(45 ± 37)	1590/1625/1691	22/29/35
$15\% + 10\% + 5\%$	(47 ± 45)	1556/1609/1669	23/29/39
$10\% \times 3$	(35 ± 43)	1551/1616/1680	22/29/37
$5\% \times 6$	(34 ± 32)	1558/1600/1646	20/30/36

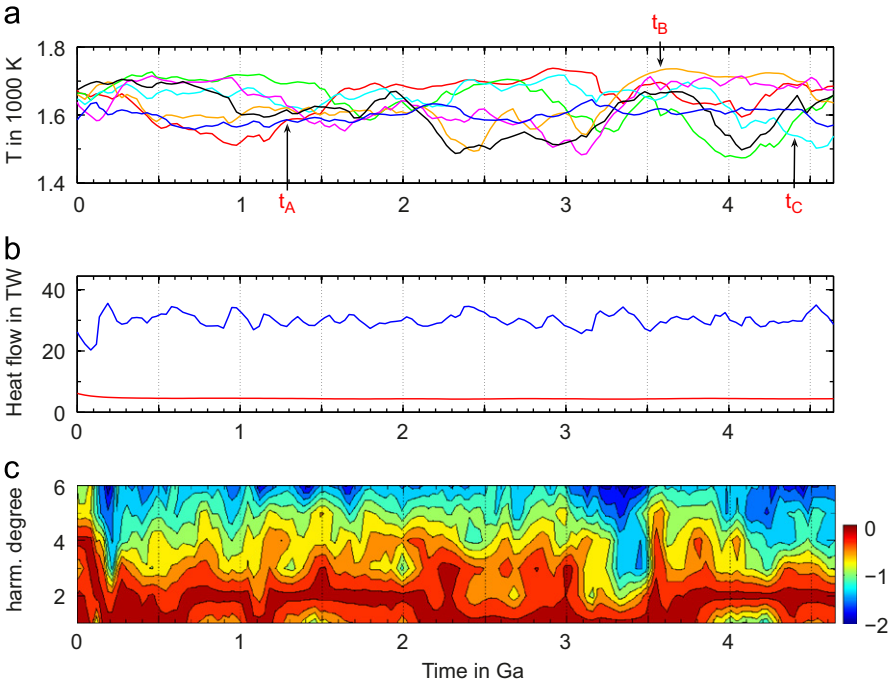

Fig. 4. As Fig. 3, but for the case with six smaller continents. (a) The blue curve displays the suboceanic temperature. The other curves represent the temperatures below individual continents. Different colors are related to the number labels given in Fig. 2 as follows: (1) red, (2) green, (3) orange, (4) cyan, (5) black, (6) magenta. Labels t_A, t_B and t_C mark the configurations in Fig. 2. (b) Oceanic heat flow (blue) and total continental heat flow (red). (c) Heterogeneity spectrogram of the temperature field as in Fig. 3c. (For interpretation of the references to color in this figure caption, the reader is referred to the web version of this article.)

from the influence of subduction of cold oceanic material, which results in a general warming under the supercontinent and particularly below its center, i.e. below continent '3'.

The warming effect of a supercontinent assembly is illustrated in Fig. 5, where the mean suboceanic temperature is compared to the mean subcontinental temperature for a time period that starts before the formation of the supercontinent and lasts until continents have dispersed again (Fig. 5a). At time $t_{-2} \approx 2.85$ Ga the continents are dispersed and the temperature of the subcontinental mantle is only slightly higher than the temperature of the suboceanic mantle (Fig. 5b). After that, continents start to assemble over a cold downwelling, such that the subcontinental mantle cools slightly ($t_{-1} \approx 3.18$ Ga, Fig. 5c). However, once supercontinent assembly is completed warming of subcontinental mantle sets in and the warmest state is reached about 400 Ma later, lasting about 200 Ma (Fig. 5d) before the first break-up events occur at time $t_{+1} \approx 3.81$ Ga (Fig. 5e). This leads to cooling of subcontinental mantle and when the former supercontinent has split into two dispersed fragments of three continents at time $t_{+2} \approx 4.07$ Ga (Fig. 5f), the average subcontinental mantle is about 100 K colder than at its hottest state. The total duration of the supercontinent event (dispersed–assembled–dispersed) is about 1.2 Ga, longer than expected on Earth, which is not surprising, because our models are simplified (for instance, basal heating and depth-dependent viscosity have been neglected here).

During this dispersed state, or even when the two fragments reassemble and build an elongated chain rather than a compact supercontinent (like at time $t_C \approx 4.4$ Ga, Fig. 2c), the mantle below individual continents can be significantly colder than the average suboceanic mantle. For instance, the temperature below continent '4', which builds one end of the continent chain in Fig. 2c, is about 80 K lower than that below the oceanic regions. Due to the low degree of connectivity (only one other continent is connected to continent '4') the formation of a subduction zone that almost surrounds this continent cannot be hindered, which finally cools the mantle below continent '4'.

So far we have only used two example configurations to describe the relationship between the connectivity of continents and the temperature below continents, but to obtain a statistically more robust finding all continent configurations that occur in this simulation should be considered. We use the angular distance between each pair of continents as a time-dependent proxy for the continent configuration. Thus, the degree of connectivity of each of the six continents is described by the evolution of the angular distances α_{norm} to the five neighboring continents (the time series of all angular distances is presented in Fig. A2 in Appendix). The mean value $\overline{\alpha}_{norm}$ of these angular distances at a given time measures the average angular distance of a continent to its neighbors: the smaller the mean angular distance is, the more closely the continents are assembled. Consequently, it will be smallest for a compact supercontinent configuration. Along with this calculation of $\overline{\alpha}_{norm}$, the temperature below individual continents is monitored as has already been shown in Fig. 4a. Thus, we obtain a data set consisting of one averaged angular distance and six subcontinental temperatures for each time step, which is then used for a statistical analysis presented in Fig. 6 (see figure caption for details). Although the standard deviation of the subcontinental temperature is relatively large, a clear trend is observed: the more dispersed the continents are on average (i.e. the larger the mean angular distance is), the lower is the temperature below the continents, which indicates the importance of the continent distribution for the Earth's thermal evolution.

4. Discussion

Our models presented here are a next step towards a geodynamic model of mantle convection consistent with global tectonics. They first confirm that previous results obtained with plate-like behavior but in 2D (Lenardic et al., 2011), or in 3D geometry but without plate-like behavior (Coltice et al., 2007;

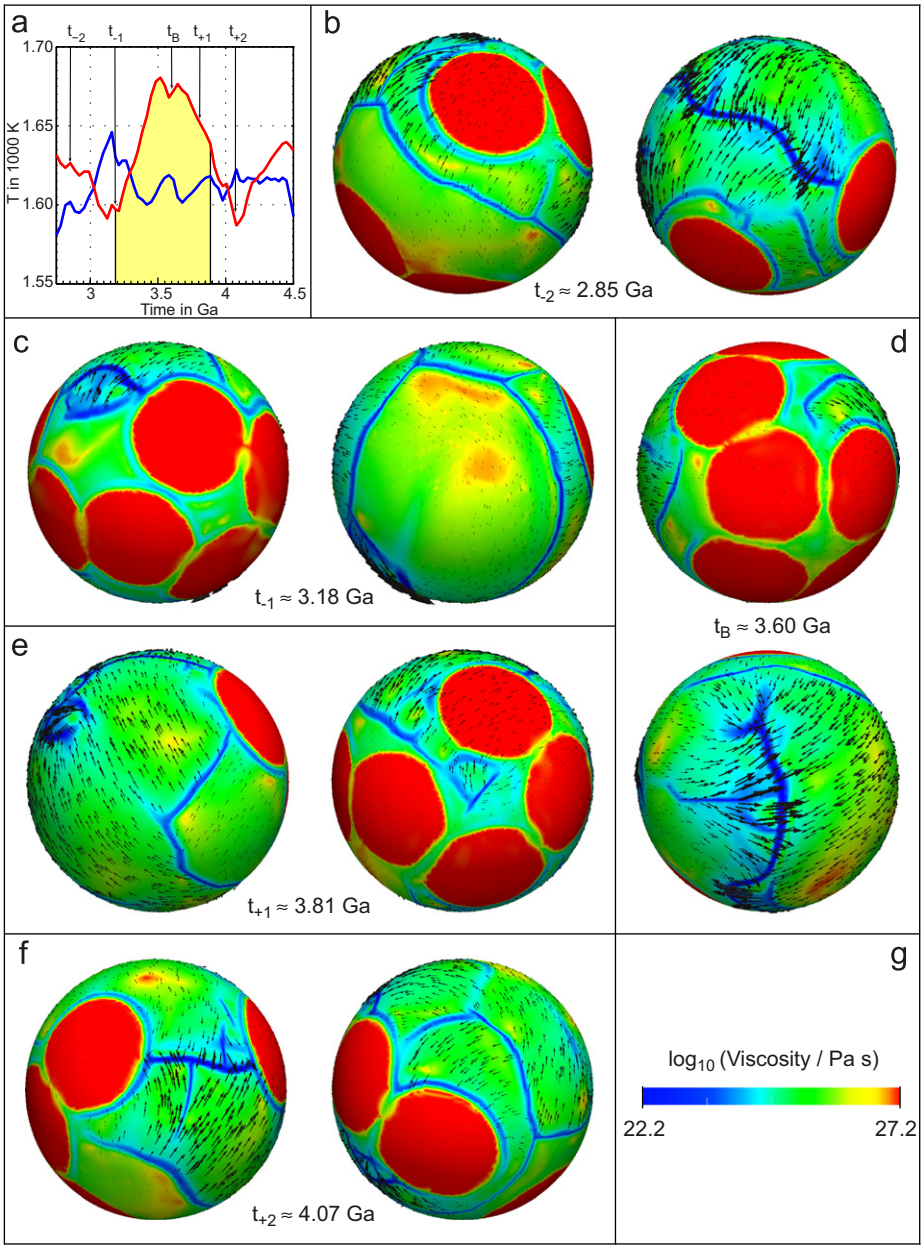

Fig. 5. Detailed analysis of a supercontinent event. (a) Zoom-in of the time series of suboceanic (blue) and mean subcontinental temperature (red). The approximate period when a compact supercontinent exists is indicated by the shaded yellow area under the graph. Labels $t_{-2},\ldots,t_{+2}$ indicate points in time that correspond to (b)–(f), respectively. (b)–(f) Snapshots of the viscosity field as in Fig. 2 at different stages of the supercontinent event. (g) Colorbar for the viscosity field. (For interpretation of the references to color in this figure caption, the reader is referred to the web version of this article.)

Phillips and Coltice, 2010), still hold: mantle temperature below a supercontinent is statistically higher by >50 K than below dispersed continents. However, they also show that changes in surface tectonics have a strong impact on the thermal evolution below continents and oceans. In the supercontinent configuration, our calculations show that most of the temporal evolution of mantle temperature depends on the dynamics in the oceanic area. When new instabilities and plate boundaries are generated the heat flow is maximum and the suboceanic temperature decreases while that below the supercontinent increases. When the supercontinent is stable, dynamics in the oceanic area is only slightly constrained by the presence of the continent. When the shape of the supercontinent is chain-like, strong temperature gradients below the center and the edges exist. The mantle underneath continental boundaries can be colder by as much as 15% than the mantle underneath the center of continents. A continent focusses the heat below its center, such that the mantle below the continent center, which is also the center of the chain-structure, is the hottest. The hot material then flows laterally towards the edges of the chain-structure and slowly cools by diffusion in the boundary layer (continents are not perfect insulators). As part of this flow is parallel to the axis of the continent chain, the formerly hot material has experienced a long period of cooling when it reaches the end of the chain and usually meets a cold downwelling at the ocean–continent boundary. In more compact supercontinent configurations, the period of cooling is shorter because the distance between the center and the edge is smaller.

With multiple continents, the dynamics of the oceanic regions are more constrained because the location for the onset of new cold instabilities and plate boundaries is confined to a smaller area (between several continents). Hence major tectonic changes, like complete reorganization of plate motions observed with a

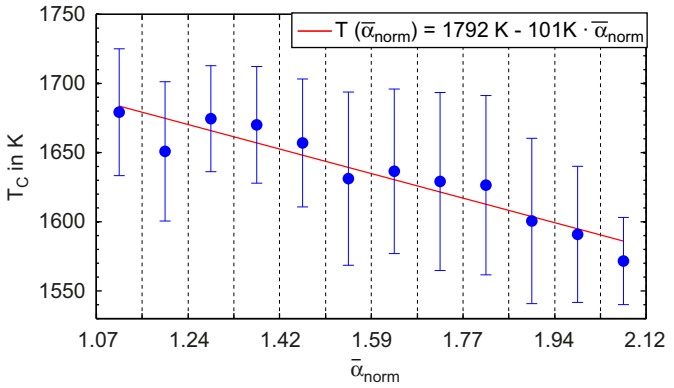

Fig. 6. Subcontinental temperature versus averaged normalized angle. For each continent and each time step the angular distance between each pair of continents is averaged to obtain one value representing the separation of the continent from each of the other five continents. The range of all occurring values has been subdivided into small bins (the bin size is indicated by the dashed vertical grid lines). Blue dots represent the mean value of subcontinental temperatures that occur for angles of a specific bin and the error bars denote the corresponding standard deviation. The red line is a linear regression using a least squares method. The time series of all angular distances are given in Fig. A2 in Appendix. (For interpretation of the references to color in this figure caption, the reader is referred to the web version of this article.)

stable supercontinent, do not occur with dispersed continents. However, the continent distribution has more degrees of freedom, and as a consequence, fluctuations of the thermal field below individual continents have a higher amplitude, but fluctuations in the oceanic regions are smaller.

Plate tectonic reconstructions are rather limited because only the last 150 Ma are well accessible (e.g. Engebretson et al., 1984; Scotese, 1991; Deparis et al., 1995; Lithgow-Bertelloni and Richards, 1998; Torsvik et al., 2010). Hence it is difficult to compare the thermal predictions of our model to long-term observations. However, one indication is the residual roughness of the seafloor, which does not account for the effects of spreading rate and is therefore appropriate to examine the role of mantle temperature on the seafloor roughness. The residual roughness in the Central Atlantic is anomalously low (Whittaker et al., 2008). This may be explained by the formation of the local Cretaceous crust from the hot mantle below Pangaea: a large-scale thermal anomaly would tend to create a thicker than normal crust with reduced brittle fracturing and consequently lower seafloor roughness. Evidence for a significantly hotter mantle below Pangaea is, for instance, given by the emplacement of the Central Atlantic Magmatic Province (see Coltice et al., 2007). After the initial break-up of Pangaea the temperature anomaly took about 100 Ma to vanish by thermal diffusion through the Atlantic seafloor (Whittaker et al., 2008). These observations are consistent with our simulations that predict hotter subcontinental mantle below a compact supercontinent. The reconstructions of the oceanic heat flow suggest rather high heat flow after the break-up of Pangaea followed by a steady decrease of around 15% since 80 Ma ago (Loyd et al., 2007; Becker et al., 2009). These numbers fall in the range predicted by our models with multiple continents, and we expect a period of cooling below continents and oceans right after the break-up.

According to our models, the present-day tectonic configuration would generate limited temperature differences between continents and oceans, and between individual continents. Eventually, the mantle below the largest continents and plates would be the hottest because of less efficient cooling. The thickness of the transition zone provides a proxy to study the temperature within the upper mantle, although some variations cannot be attributed to purely thermal effects. The recent work of Houser et al. (2008) suggests that there is no systematic thinning of the transition zone below oceans or continents. Hence, the subcontinental mantle is not significantly hotter than the suboceanic mantle in the present-day situation. The hotter regions (i.e. places where the transition zone is thinner) are below the Pacific, Africa and Asia, which are the bigger plates and continents. However, our models do not include plumes, which may contribute significantly to local thinning of the transition zone.

Our models give a possible explanation for the suggested episodicity in growth of continental crust (e.g. Condie, 2004; Pearson et al., 2007). These episodes of crustal growth are likely to correlate with melting under the continents, i.e. high excess temperatures below the continents. In our models these excess temperatures are strongly varying in time in response to changes in continent configuration. Thus, the temperature below a certain continent will exceed the solidus temperature only during episodes of continental aggregation.

Although our models give a deeper insight into the link between the thermal and tectonic history of the Earth's mantle, they are still rather simplified, so here we briefly discuss the major shortcomings, which will be improved in future studies. First, our assumption of an entirely internally heated mantle is certainly not true for the Earth, but it is a first-order approximation of the Earth's mantle (e.g. Davies, 1988; Sleep, 1990; Turcotte and Schubert, 2002). However, active upwellings due to basal heating could have important effects on the thermal field of the mantle and might lead to a less pronounced or even vanishing temperature excess below continents. For instance, Heron and Lowman (2010, 2011) do not report a significant temperature excess below continents and no preference of plumes to form under continents as observed in various earlier studies (e.g. Gurnis, 1988; Zhong and Gurnis, 1993; Lowman and Gable, 1999; Yoshida et al., 1999; Zhong et al., 2007; O'Neill et al., 2009). They explain their observation by the dominance of the lateral size of a tectonic plate on the temperature below this plate, regardless of whether an oceanic or a continental plate. However, their results are obtained with prescribed oceanic and continental plates that both have the same thickness and are therefore not representative of Earth.

Strong plumes from the lower mantle might also affect the timescale of continental aggregation (Phillips and Bunge, 2007). This would give a possible explanation why the timescale of aggregation in our presented model is significantly longer than the expected 300–500 Ma for the Earth (e.g. Zhong and Gurnis, 1993). However, this time scale is not well constrained, especially for supercontinents prior to Pangaea, as the tectonic history is well-known only for the last 150 Ma (Lithgow-Bertelloni and Richards, 1998). Additionally, deviant time scales could also be explained by the simplified viscosity profile in our models, for instance the omission of a depth dependence, or the usage of a smaller than Earth-like Rayleigh number (due to computational reasons).

Finally, continents on Earth are not completely resistant against deformation and can rift, which is not the case in our models. Plumes, which may erode the base of the lithosphere and induce additional stresses could make continental rifting easier (Storey, 1995; Santosh et al., 2009), although it is still under debate if plumes constitute a major driving force of continental rifting (e.g. Lowman and Jarvis, 1996, 1999; Li et al., 2008). Break-up could alternatively be enhanced by using more deformable continents in our models. So far, we have treated continents as strong cratons that hardly deform. Weaker rheology would lead to greater continental deformation, but also to more efficient subduction and recycling of continental material (e.g. Lenardic and Moresi, 1999; Lenardic et al., 2003), which is not suitable for investigating the long-term thermal history of the mantle. A possible reconciliation is the inclusion of weaker mobile belts that protect the continental

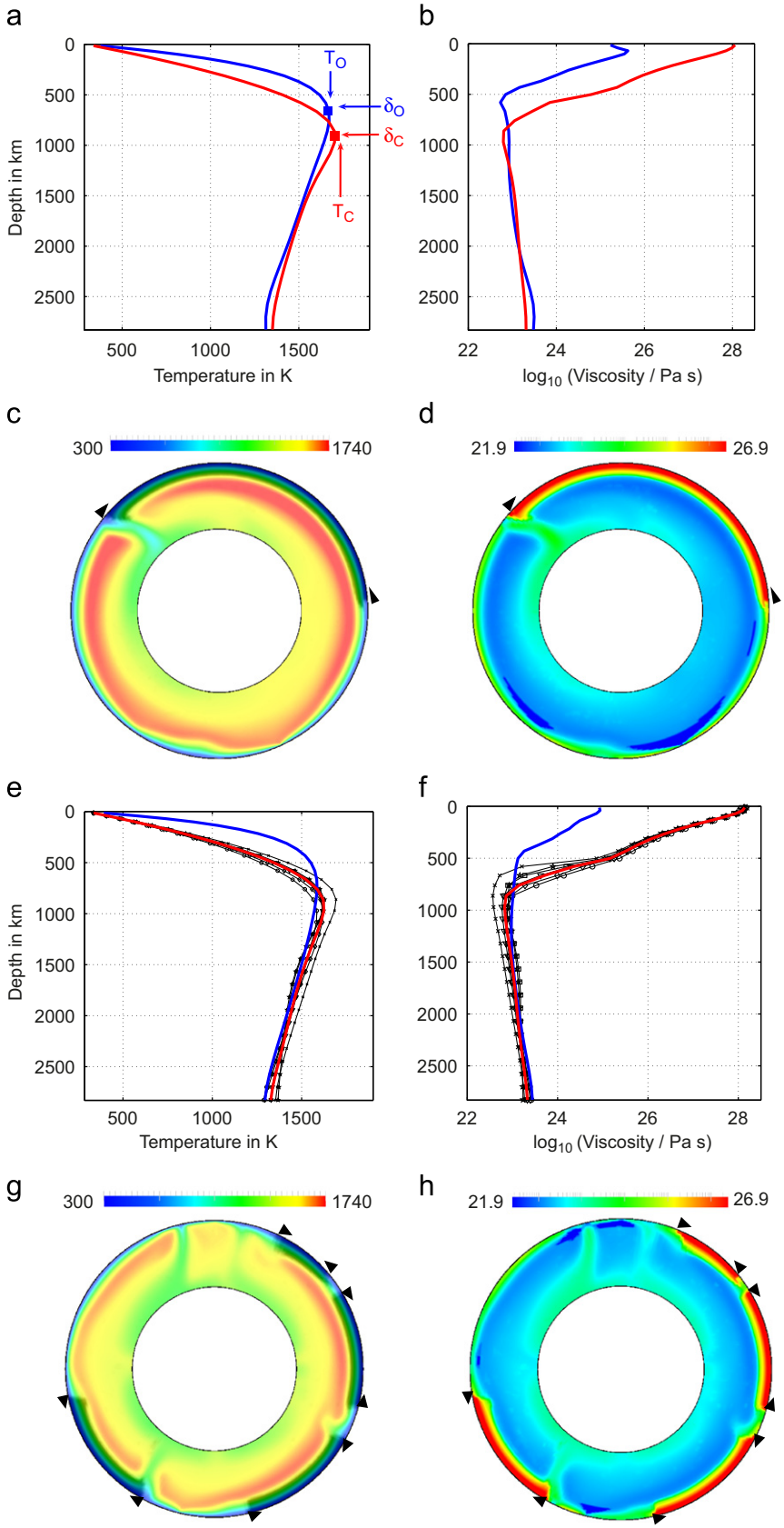

Fig. A1. Radial mantle structure: (a) Horizontally averaged radial temperature profile, separated into oceanic (blue) and continental regions (red) for the case with one continent at time $t_A \approx 2.45$ Ga. The small square boxes indicate the depths (δ_O, δ_C) where suboceanic and subcontinental temperatures (T_O, T_C) are taken. (b) As in part (a), but for viscosity instead of temperature. (c)–(d) Characteristic cross-sections of the temperature and viscosity field with the color coding indicated in the respective colorbars. The black triangles mark the position of the continent. (e)–(h) are equivalent to (a)–(d), but for the case with six continents at time $t_A \approx 1.3$ Ga. In (e)–(f) the mean radial temperature and viscosity profile is plotted in red. Profiles for the individual continents are indicated by the thinner grey lines. (For interpretation of the references to color in this figure caption, the reader is referred to the web version of this article.)

interior against deformation (Lenardic et al., 2000) and could serve as sutures within a supercontinent (as in Yoshida, 2010), which are thought to be preferred locations of continental rifting (e.g. Murphy et al., 2006).

5. Conclusions

In the present study we have presented 3D spherical mantle convection simulations with self-consistently generated plates and mobile continents. We have investigated how the presence of continents affects the evolution of the Earth's mantle with regard to the thermal history below continents and oceans and its link to the tectonic history, i.e. the distribution of continental and oceanic plates. Our results can be summarized in two concluding remarks:

1. A supercontinent imposes a very long wavelength structure on the mantle flow, upon which are superposed smaller wavelength structures that are generated by the formation of new plate boundaries in the oceanic part. These new instabilities can lead to an increase in oceanic heat flow by up to 45% on a timescale of 100 Ma and a decrease in suboceanic temperature by up to almost 100 K. The position of the oceanic plate boundaries relative to the continental margin then affects the mantle temperature below the continent. A continental convection cell that contains a significant amount of oceanic seafloor is less efficient in insulating subcontinental mantle than a convection cell that is almost completely covered with the continental lid. Insulation forces subcontinental mantle to be up to ≈ 140 K hotter than suboceanic mantle, which could be sufficient to induce partial melting under a supercontinent and could lead to enhanced magmatic activity and possibly breakup (e.g. Anderson, 1982; Coltice et al., 2009).

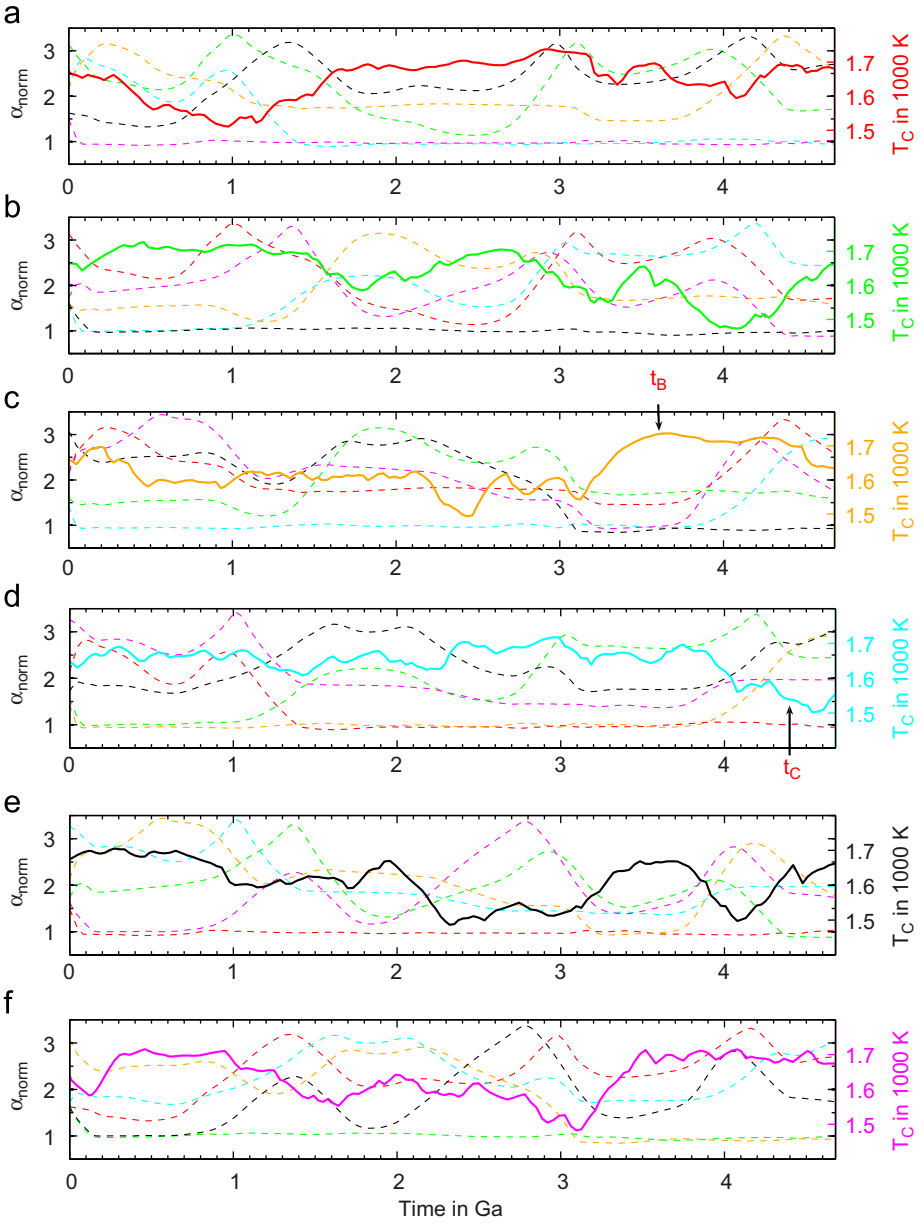

Fig. A2. Time series of the normalized angle α_{norm} between each pair of continents. The six subplots (a)–(f) show the subcontinental temperature T_C of one specific continent (bold line, using the right y-axis and the same color coding as in Fig. 4a) and the angle to all other continents (dashed lines). The angles are calculated between the center of the continents and are normalized with the continental angular diameter, such that values close to unity indicate two assembled continents and large values indicate two dispersed continents. Note that the calculation of angles is symmetric: the angle between continents i and j is identical to the angle between continents j and i. (For interpretation of the references to color in this figure caption, the reader is referred to the web version of this article.)

2. If more than one continent is considered, effects of continental aggregation and dispersal are superposed upon the trends observed with a single supercontinent. These effects lead to much stronger variations in subcontinental temperatures that are directly related to the distribution of continents. However, fluctuations of oceanic heat flow (30% variation between minimum and maximum) and suboceanic temperature ($\lesssim 5\%$ variation) are smaller than in the supercontinent case. If continents are assembled in a compact cluster (like a supercontinent), they isolate each other from subduction and inflow of colder oceanic material, which causes a heating of up to 100 K of the mantle below. If, however, the continents are dispersed or loosely connected in a chain-like structure, there is no significant warming and subcontinental mantle can even be colder than suboceanic mantle. This suggests that melting and magmatic activity below continents are episodic processes, which possibly explain the observed episodicity in the growth of continental crust (Condie, 2004; Pearson et al., 2007).

Acknowledgements

We like to thank the editor as well as Julian Lowman and an anonymous reviewer for their fruitful comments that helped to improve the initial manuscript. The research leading to these results has received funding from Crystal2Plate, a FP-7 funded Marie Curie Action under grant agreement number PITN-GA-2008-215353. Calculations were performed on ETH's Brutus high-performance computing cluster. This work was supported by a grant from the Swiss National Supercomputing Centre (CSCS) under project ID s272.

Appendix A

See Figs. A1 and A2.

Appendix B. Supplementary material

Supplementary data associated with this article can be found in the online version of http://dx.doi.org/10.1016/j.epsl.2012.07.011.

References

Anderson, D., 1982. Hotspots, polar wander, Mesozoic convection and the geoid. Nature 297, 391–393.
Becker, T., Conrad, C., Buffett, B., Müller, R., 2009. Past and present seafloor age distributions and the temporal evolution of plate tectonic heat transport. Earth Planet. Sci. Lett. 278, 233–242.
Cande, S., Stegman, D., 2011. Indian and African plate motions driven by the push force of the Reunion plume head. Nature 475, 47–52.
Chapman, C., Childress, S., Proctor, M., 1980. Long wavelength thermal convection between non-conducting boundaries. Earth Planet. Sci. Lett. 51, 362–369.
Coltice, N., Bertrand, H., Rey, P., Jourdan, F., Phillips, B., Ricard, Y., 2009. Global warming of the mantle beneath continents back to the Archaean. Gondwana Res. 15, 254–266.
Coltice, N., Phillips, B., Bertrand, H., Ricard, Y., Rey, P., 2007. Global warming of the mantle at the origin of flood basalts over supercontinents. Geology 35, 391–394.
Coltice, N., Rolf, T., Tackley, P.J., Labrosse, S., 2012. Dynamic causes of the relation between area and age of the ocean floor. Science 336, 335–338.
Condie, K., 2004. Supercontinents and superplume events: distinguishing signals in the geologic record. Phys. Earth Planet. Int. 146, 319–332.
Cooper, C., Lenardic, A., Moresi, L.N., 2006. Effects of continental insulation and the partitioning of heat producing elements on the Earth's heat loss. Geophys. Res. Lett. 33, L13313.
Davies, G., 1988. Ocean bathymetry and mantle convection 1. Large-scale flow and hotspots. J. Geophys. Res. 93, 10467–10480.
Deparis, V., Legros, H., Ricard, Y., 1995. Mass anomalies due to subducted slabs and simulations of plate motion since 200 my. Phys. Earth Planet. Int. 89, 271–280.
Engebretson, D., Cox, A., Gordon, R., 1984. Relative motions between oceanic plates of the pacific basin. J. Geophys. Res. 89, 10291–10310.
Gait, A.D., Lowman, J.P., 2007. Time-dependence in mantle convection models featuring dynamically evolving plates. Geophys. J. Int. 171, 463–477.
Grigné, C., Labrosse, S., Tackley, P., 2005. Convective heat transfer as a function of wavelength: implications for the cooling of the Earth. J. Geophys. Res. 110, B03409.
Grigné, C., Labrosse, S., Tackley, P., 2007. Convection under a lid of finite conductivity in wide aspect ratio models: effect of continents on the wavelength of mantle flow. J. Geophys. Res. 112, B08403.
Guillou, L., Jaupart, C., 1995. On the effect of continents on mantle convection. J. Geophys. Res. 100, 24217–24238.
Gurnis, M., 1988. Large-scale mantle convection and the aggregation and dispersal of supercontinents. Nature 332, 695–699.
Gurnis, M., Zhong, S., 1991. Generation of long wavelength heterogeneity in the mantle by the dynamic interaction between plates and convection. Geophys. Res. Lett. 18, 581–584.
van Heck, H., Tackley, P., 2008. Planforms of self-consistently generated plates in 3d spherical geometry. Geophys. Res. Lett. 35, L19312.
Heron, P., Lowman, J., 2010. Thermal response of the mantle following the formation of a "super-plate". Geophys. Res. Lett. 37, L22302.
Heron, P., Lowman, J., 2011. The effects of supercontinent size and thermal insulation on the formation of mantle plumes. Tectonophysics 510, 28–38.
Hirth, G., Kohlstedt, D.L., 1996. Water in the oceanic upper mantle: implications for rheology, melt extraction and the evolution of the lithosphere. Earth Planet. Sci. Lett. 144, 93–108.
Hoeink, T., Lenardic, A., 2010. Long wavelength convection, Poiseuille–Couette flow in the low-viscosity asthenosphere and the strength of plate margins. Geophys. J. Int. 180, 23–33.
Houser, C., Masters, G., Flanagan, M., Shearer, P., 2008. Determination and analysis of long-wavelength transition zone structure using SS precursors. Geophys. J. Int. 174, 178–194.
Karato, S.-I., 2010. Rheology of the deep upper mantle and its implication for the preservation of the continental roots: a review. Tectonophysics 481, 82–98.
Lenardic, A., Jellinek, A., O'Neill, C., Cooper, C., Moresi, L., Lee, C., 2011. Continents, supercontinents, mantle thermal mixing and mantle thermal isolation: theory, numerical simulations, and laboratory experiments. Geochem. Geophys. Geosyst. 12, Q10016.
Lenardic, A., Moresi, L.N., 1999. Some thoughts on the stability of cratonic lithosphere: effects of buoyancy and viscosity. J. Geophys. Res. 104, 12747–12758.
Lenardic, A., Moresi, L.N., Jellinek, A., Manga, M., 2005. Continental insulation, mantle cooling, and the surface area of oceans and continents. Earth Planet. Sci. Lett. 234, 317–333.
Lenardic, A., Moresi, L.N., Mühlhaus, H., 2000. The role of mobile belts for the longevity of deep cratonic lithosphere: the crumple zone model. Geophys. Res. Lett. 27, 1235–1238.
Lenardic, A., Moresi, L.N., Mühlhaus, H., 2003. Longevity and stability of cratonic lithosphere: insights from numerical simulations of coupled mantle convection and continental tectonics. J. Geophys. Res. 108. (ETG 9).
Lenardic, A., Moresi, M., 2001. Heat flow scaling for mantle convection below a conducting lid: resolving seemingly inconsistent modeling results regarding continental heat flow. Geophys. Res. Lett. 28, 1311–1314.
Li, Z., et al., 2008. Assembly, configuration, and break-up history of Rodinia: a synthesis. Precambrian Res. 160, 179–210.
Lithgow-Bertelloni, C., Richards, M., 1998. The dynamics of cenozoic and mesozoic plate motions. Rev. Geophys. 36, 27–78.
Lowman, J., Gable, C., 1999. Thermal evolution of the mantle following continental aggregation in 3d convection models. Geophys. Res. Lett. 26, 2649–2652.
Lowman, J., Jarvis, G., 1995. Mantle convection models of continental collision and breakup incorporating finite thickness plates. Phys. Earth Planet. Int. 88, 53–68.
Lowman, J., Jarvis, G., 1996. Continental collisions in wide aspect ratio and high Rayleigh number two-dimensional mantle convection models. J. Geophys. Res. 101, 25485–25497.
Lowman, J., Jarvis, G., 1999. Effects of mantle heat source distribution on supercontinent stability. J. Geophys. Res. 104, 12733–12746.
Lowman, J.P., King, S.D., Gable, C.W., 2001. The influence of tectonic plates on mantle convection patterns, temperature and heat flow. Geophys. J. Int. 146, 619–636.
Loyd, S., Becker, T., Conrad, C., Lithgow-Bertelloni, C., Corsetti, F., 2007. Time-variability in Cenozoic reconstructions of mantle heat flow: plate tectonic cycles and implications for Earth's thermal evolution. Proc. Natl. Acad. Sci. USA 104, 14,266–14,271.
McHone, J., 2000. Non-plume magmatism and rifting during the opening of the central Atlantic Ocean. Tectonophysics 316, 287–296.
McNamara, A., Zhong, S., 2005. Degree-one mantle convection: dependence on internal heating and temperature-dependent rheology. Geophys. Res. Lett. 32, L01301.
Moresi, L., Solomatov, V., 1998. Mantle convection with a brittle lithosphere: thoughts on the global tectonic styles of the Earth and Venus. Geophys. J. Int. 133, 669–682.
Murphy, J., Gutierrez-Alonso, G., Nance, R., Fernandez-Suarez, J., Keppie, J., Quesada, C., Strachan, R., Dostal, J., 2006. Origin of the Rheic ocean: rifting along a neoproterozoic suture? Geology 34, 325–328.
O'Neill, C., Lenardic, A., Jellinek, A., Moresi, L.N., 2009. Influence of supercontinents on deep mantle flow. Gondwana Res. 15, 276–287.

O'Neill, C., Lenardic, G., O'Reilly, S., 2008. Dynamics of cratons in an evolving mantle. Lithos 102, 12–24.
Pearson, D., Parman, S., Nowell, G., 2007. A link between large mantle melting events and continent growth seen in osmium isotopes. Nature 449, 203–205.
Phillips, B., Bunge, H.P., 2005. Heterogeneity and time dependence in 3d spherical mantle convection models with continental drift. Earth Planet. Sci. Lett. 233, 121–135.
Phillips, B., Bunge, H.P., 2007. Supercontinent cycles disrupted by strong mantle plumes. Geology 35, 847–850.
Phillips, B., Coltice, N., 2010. Temperature beneath continents as a function of continental cover and convective wavelength. J. Geophys. Res. 115, B04408.
Poudjom Djomani, Y.H., O'Reilly, S.Y., Griffin, W.L., Morgan, P., 2001. The density structure of subcontinental lithosphere through time. Earth Planet. Sci. Lett. 184, 605–621.
Rolf, T., Tackley, P., 2011. Focussing of stress by continents in 3D spherical mantle convection with self-consistent plate tectonics. Geophys. Res. Lett. 38, L18301.
Santosh, M., Maruyama, S., Yamamoto, S., 2009. The making and breaking of supercontinents: some speculations based on superplumes, super downwelling and the role of tectosphere. Gondwana Res. 15, 324–341.
Scotese, C., 1991. Jurassic and Cretaceous plate tectonic reconstructions. Palaeogeogr. Palaeocl. 87, 493–501.
Sleep, N., 1990. Hotspots and mantle plumes: some phenomenology. J. Geophys. Res. 95, 6715–6736.
Solomatov, V., 1995. Scaling of temperature- and stress-dependent viscosity convection. Phys. Fluids 7, 266–274.
Stein, C., Lowman, J.P., 2010. Response of mantle heat flux to plate evolution. Geophys. Res. Lett. 37, L24201.
Storey, B., 1995. The role of mantle plumes in continental breakup: case histories from Gondwanaland. Nature 377, 301–308.
Tackley, P., 1996. On the ability of phase transitions and viscosity layering to induce long wavelength heterogeneity in the mantle. Geophys. Res. Lett. 23, 1985–1988.
Tackley, P., 2000a. Self-consistent generation of tectonic plates in time-dependent, three-dimensional mantle convection simulations, 1. Pseudoplastic yielding. Geochem. Geophys. Geosyst. 1 2000GC000036.
Tackley, P., 2000b. Self-consistent generation of tectonic plates in time-dependent, three-dimensional mantle convection simulations 2. Strain weakening and asthenosphere. Geochem. Geophys. Geosyst. 1 2000GC000043.
Tackley, P., 2008. Modelling compressible mantle convection with large viscosity contrasts in a three-dimensional spherical shell using the Yin-Yang grid. Phys. Earth Planet. Int. 171, 7–18.
Tackley, P., King, S., 2003. Testing the tracer ratio method for modeling active compositional fields in mantle convection simulations. Geochem. Geophys. Geosyst. 4 2001GC00214.
Torsvik, T., Steinberger, B., Gurnis, M., Gaina, C., 2010. Plate tectonics and net lithosphere rotation over the past 150 My. Earth Planet. Sci. Lett. 291, 106–112.
Trubitsyn, V., Mooney, W., Abbott, D., 2003. Cold Cratonic roots and thermal blankets: how continents affect mantle convection. Int. Geol. Rev. 45, 479–496.
Turcotte, D., Schubert, G., 2002. Geodynamics, 2nd ed. Cambridge University Press, Cambridge.
Whittaker, J., Müller, R., Roest, W., Wessel, P., Smith, W., 2008. How supercontinents and superoceans affect seafloor roughness. Nature 456, 938–942.
Yoshida, M., 2008. Mantle convection with longest-wavelength thermal heterogeneity in a 3-d spherical model: degree one or two? Geophys. Res. Lett. 35, L23302.
Yoshida, M., 2010. Preliminary three-dimensional model of mantle convection with deformable, mobile continental lithosphere. Earth Planet. Sci. Lett. 295, 205–218.
Yoshida, M., Iwase, Y., Honda, S., 1999. Generation of plumes under a localized high viscosity lid in 3-d spherical shell convection. Geophys. Res. Lett. 26, 947–950.
Zhang, N., Zhong, S., McNamara, A., 2009. Supercontinent formation from stochastic collision and mantle convection models. Gondwana Res. 15, 267–275.
Zhong, S., Gurnis, M., 1993. Dynamic feedback between a continentlike raft and thermal convection. J. Geophys. Res. 98, 12219–12232.
Zhong, S., Zhang, N., Li, Z., Roberts, J., 2007. Supercontinent cycles, true polar wander, and very long-wavelength mantle convection. Earth Planet. Sci. Lett. 261, 551–564.